



PERGAMON

Building and Environment 36 (2001) 493–501

BUILDING AND  
ENVIRONMENT

www.elsevier.com/locate/buildenv

# Natural ventilation in an enclosure induced by a heat source distributed uniformly over a vertical wall

Z.D. Chen\*, Y. Li, J. Mahoney

*Advanced Thermo-Fluids Technologies Laboratory, CSIRO Building, Construction and Engineering, PO Box 56, Highett, Victoria 3190, Australia*

Received 23 August 1999; received in revised form 15 November 1999; accepted 26 January 2000

## Abstract

A simple multi-layer stratification model is suggested for displacement ventilation in a single-zone building driven by a heat source distributed uniformly over a vertical wall. Theoretical expressions are obtained for the stratification interface height and ventilation flow rate and compared with those obtained by an existing model available in the literature. Experiments were also carried out using a recently developed fine-bubble modelling technique. It was shown that the experimental results obtained using the fine-bubble technique are in good agreement with the theoretical predictions. © 2000 Elsevier Science Ltd. All rights reserved.

*Keywords:* Natural ventilation; Vertical wall; Constant heat flux

## 1. Introduction

Displacement ventilation flows in a building due to heated vertical walls are of practical importance for building designs. However, few investigations have been carried out in this area. Linden et al. [1] proposed a multi-layer stratification model for displacement ventilation driven by a vertically distributed buoyancy source. The flow field in the building was divided into several horizontal layers. With the assumption of equal depth for all the layers, solutions for the depth of layers, the flow rate through openings and the reduced gravity were obtained for a vertical line with constant buoyancy flux (corresponding to constant heat flux). Linden et al. [1] also carried out experiments using a salt-bath modelling system. It was shown that although there were indications of the possible existence of multi-layer stratification, results essentially showed a two-layer stratification with an approximately linear salt concentration distribution in the

upper layer. Comparisons between experimental results and theoretical predictions have not been reported for the vertically distributed source in their work.

Cooper et al. [2] carried out experiments of displacement ventilation due to a vertical wall source using a salt-bath modelling system. The distributions of salt concentration reported by Cooper et al. [2] show similar trends to that of Linden et al. [1] for a vertical line source. From both the experiments by Linden et al. [1] and Cooper et al. [2] it appears that multi-layer stratification may exist in the case of vertical distributed sources. However, stratifications above the bottom layer are very weak. Linden et al. [1] suggested that a significant amount of vertical mixing may contribute to the smoothing out of the stratifications in the upper layer.

In this work, a simple multi-layer stratification model is proposed and analytical predictions for the interface height and ventilation flow rate are compared with those obtained by Linden's approach. Experiments were also carried out using a recently developed fine-bubble modelling technique, and results obtained for the stratification interface height are compared

\* Corresponding author. Tel.: +61-3-9252-6335; fax: +61-3-9252-6251.

## Nomenclature

$a_1$	top opening area per unit width [m]
$a_2$	bottom opening area per unit width [m]
$A_w^*$	effective opening area per unit width, $A^* = a_1 a_2 / [\frac{1}{2}(a_1^2/c_2 + a_2^2/c_1)]^{1/2}$ [m]
$B_w$	buoyancy flux per unit area [ $\text{m}^2 \text{s}^{-3}$ ]
$c_1$	discharge coefficient of the top opening
$c_2$	discharge coefficient of the bottom opening
$C_p$	thermal capacity of the ambient air [J/kg K]
$F$	constant, $F = (3\alpha/4)(4/5\alpha)^{1/3}$
$g$	gravitational acceleration [ $\text{m/s}^2$ ]
$g'_z$	reduced gravity at $z$ -level [ $\text{m/s}^2$ ]
$h$	bottom layer depth for the present model or the depth of the layers in the model of Linden et al. [m]
$H$	total height of the building [m]
$M$	flow rate in the turbulent plume per unit width [ $\text{m}^2/\text{s}$ ]
$q_w$	heat flux from a heat source [ $\text{W/m}^2$ ]
$Q$	volume flux per unit width through the bottom opening [ $\text{m}^2/\text{s}$ ]
$Q_g$	gas flow rate per unit area [m/s]
$Q_z$	total vertical flow rate per unit width at $z$ -level

	[ $\text{m}^2/\text{s}$ ]
$T_0$	temperature of the ambient air [K]
$T_z$	temperature of the air at $z$ -level [K]
$z$	vertical coordinate [m]

### Greek symbols

$\alpha$	turbulent entrainment constant
$\Delta g'$	change of the reduced gravity between adjacent layers [ $\text{m/s}^2$ ]
$\Delta Q$	volume increase rate per unit area due to a heat source [m/s]
$\Delta T$	change of the temperature between adjacent layers [K]
$\rho$	density of the ambient fluid [ $\text{kg/m}^3$ ]
$\rho_g$	density of hydrogen gas [ $\text{kg/m}^3$ ]
$\xi$	ratio between the interface height and the building height, $\xi = h/H$

### Subscripts

$i$	interface level
$z$	$z$ -level

with the theoretical predictions, as well as the experimental data available in the literature.

## 2. Extension of Linden's model

Fig. 1 shows a schematic view of displacement ventilation in a single-zone building driven by a heat source distributed uniformly over a vertical wall. The building has a bottom opening at floor level and a top opening at ceiling level. The buoyancy plume generated by the heat source entrains the fluid around it and rises to the

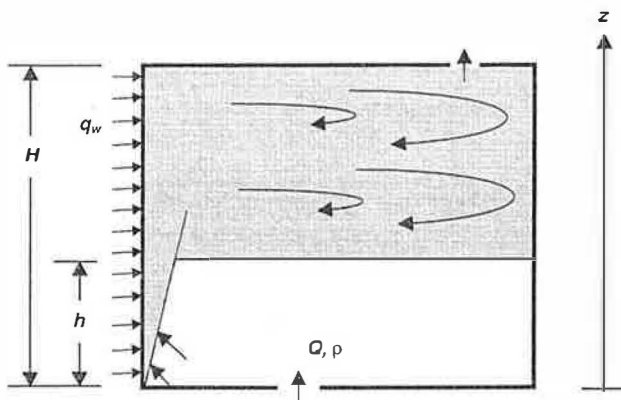


Fig. 1. Schematic view of displacement natural ventilation in a single-zone building induced by a heat source distributed uniformly over a vertical wall.

upper region of the building. Similar to displacement ventilation driven by a point or a line source, at steady state, a stratification interface forms between the dense fresh air and the upper layer of light heated air, as shown in Fig. 1. However, in the case of a vertically distributed wall source, there is a possibility of additional stratifications being formed in the upper layer, since the buoyancy source above the interface may induce further stratifications.

Linden et al. [1] suggested a multi-layer stratification model and their analysis was carried out for a vertical line source. Here, the same approach used by Linden et al. [1] will be extended to the case of a vertical wall source. Fig. 2 shows a schematic view of the multi-layer model suggested by Linden et al. [1]. It is assumed that the fluid in the plume from a lower level stratification layer, say layer 2, upon reaching its adjacent higher level stratification layer, i.e. layer 3, will be totally de-entrained and mixed within layer 3. In this case, a new buoyancy plume will be established at layer 3 and will entrain fluid towards layer 4. If we assume that there is no fluid exchange across the stratification interface outside the plume, then the density of the fluid in layer 3 outside the buoyancy plume should be the same as that in the plume from layer 2 at the interface level.

For simplicity, it is also assumed that:

- The fluid is incompressible.

• The  
be

Thes  
the  
we h

$Q_z =$

wher  
thro  
volu  
from  
the f  
flow  
Con:  
total  
cons  
that  
shou  
of ea

F1  
is al  
in ti  
can

$\Delta g'$

wher  
area  
For  
vati  
expr

$Q =$

$\frac{u_1^2}{2c_1}$

wher

$q_w$

Fig.  
indu  
Lind

- There is no change in volume during the mixing between fluids with different densities.

These two assumptions ensure volume conservation in the system. Consequently, for any horizontal level  $z$ , we have:

$$Q_z = Q + z\Delta Q \tag{1}$$

where  $Q$  is the volume flow rate per unit width through the bottom opening and  $\Delta Q = q_w/\rho C_p T_0$  is the volume increase rate per unit area due to the heat flux from the wall. Usually, the volume increase rate due to the heat flux is very small in comparison to the volume flow rate through the bottom opening, i.e.  $z\Delta Q \ll Q$ . Consequently,  $Q_z \approx Q$ . Thus, in the steady state, the total vertical volume flow rate,  $Q_z$ , is approximately constant through any horizontal plane. Considering that the flow rate in the turbulent plume in each layer should be the same at each interface level, the height of each layer must be the same except the top layer.

Further, by assuming that the depth of the top layer is also equal to the height of other layers, the change in the reduced gravity between adjacent layers,  $\Delta g'$ , can be expressed by the following equation:

$$\Delta g' = B_w h / Q \tag{2}$$

where  $B_w = q_w g / \rho C_p T_0$  is the buoyancy flux per unit area due to the heat source; and  $h$  is the layer depth. For such a multi-layer stratification system, the conservation of volume flux and Bernoulli's theorem can be expressed by the following two equations:

$$Q = u_1 a_1 = u_2 a_2 \tag{3}$$

$$\frac{u_1^2}{2c_1} + \frac{u_2^2}{2c_2} = \frac{B_w h^2 N(N+1)}{2Q} \tag{4}$$

where  $u_1$  and  $u_2$  are the flow velocity through the top

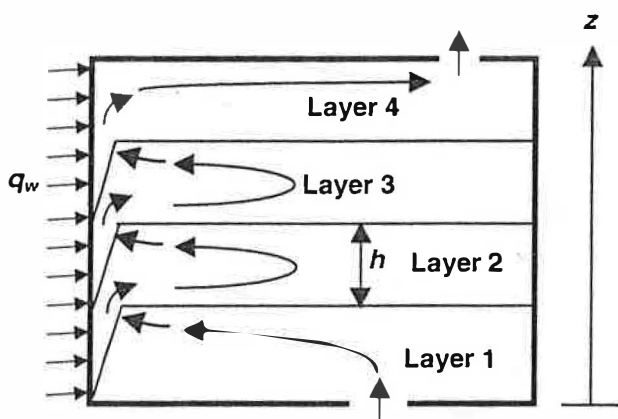


Fig. 2. Multi-layer stratification model for displacement ventilation induced by a vertically distributed buoyancy source suggested by Linden et al. [1].

and bottom opening, respectively;  $c_1$  and  $c_2$  are the corresponding discharge coefficients; and  $N = H/h - 1$  is the number of stratification interfaces. The volume flux per unit width through the bottom opening can be obtained from Eqs. (3) and (4):

$$Q = A_w^* \left[ \frac{B_w h^2 N(N+1)}{2Q} \right]^{1/2} \tag{5}$$

where  $A_w^*$  is the effective opening area per unit width,  $A_w^* = a_1 a_2 / [\frac{1}{2}(a_1^2/c_2 + a_2^2/c_1)]^{1/2}$ .

It should be noted that Eq. (5) is only valid when  $N > 1$ . For  $0 < N \leq 1$ , the system actually reduces to two-layer stratification. In this case, the depth of the bottom and top layers become  $h = H(N+1)$  and  $H-h$ , respectively. In accordance with the approach of Linden et al., the density in the top layer is equal to that in the plume at the interface level. In this case, the change of the reduced gravity between the top and the bottom layers can still be expressed by Eq. (2). However, the volume flux per unit width through the openings becomes:

$$Q = A_w^* \left[ \frac{B_w h(H-h)}{Q} \right]^{1/2} = A_w^* \left( \frac{B_w N h^2}{Q} \right)^{1/2} \tag{6}$$

For a vertical wall with a constant buoyancy flux per unit area  $B_w$ , the flow rate in the turbulent plume at an interface level  $h$  can be shown to be [3]:

$$M = FB_w^{1/3} h^{4/3} \tag{7}$$

where  $F = (3\alpha/4)(4/5\alpha)^{1/3}$  and  $\alpha$  is the turbulent entrainment constant. By matching the volume flux through openings, i.e. Eqs. (5) and (6), with the flow rate in the plume at interface level, i.e. Eq. (7), we have:

$$N(N+1)^3 = 2F^3 \frac{H^2}{A_w^{*2}} \tag{8}$$

when  $N > 1$  and

$$N(N+1)^2 = F^3 \frac{H^2}{A_w^{*2}} \tag{9}$$

when  $N \leq 1$ .

Having obtained the stratification interface position, the reduced gravity in each layer and the volume flow rate through the openings can be determined by Eqs. (2), (5) and (6). The temperature change between adjacent layers,  $\Delta T$ , can be obtained by the following relation:

$$\Delta g' = \frac{\Delta T}{T_0} g \tag{10}$$

### 3. Experimental system and qualitative observations

#### 3.1. Experimental system

Experiments for displacement ventilation in a single-zone building induced by a vertically distributed wall source were carried out by using a recently developed modelling technique, which uses fine-bubble plumes in water to simulate the buoyancy effect in buildings. Details of the modelling technique and similarity analysis can be found in our previous paper [4]. Fig. 3 shows a schematic view of the experimental system used in this work. The system consists of the following components: an inner tank; a large tank; a hydrogen bubble-generating system, which has a copper wire cathode and a graphite anode; and a constant voltage DC power supply.

The inner tank, which represented a single-zone building, had dimensions of 0.2 m (long)  $\times$  0.1 m (wide)  $\times$  0.2 m (high). There were 24 holes of 15 mm diameter on the bottom floor of the inner tank, which represented the bottom opening of the building. On the top of the inner tank, there was a sliding lid to adjust the top opening. This inner tank was situated 65 mm above the bottom floor of the large tank. The large tank, with dimensions of 0.9 m (long)  $\times$  0.345 m (wide)  $\times$  0.45 m (high), represented a static environment surrounding the building. In order to increase the electrical conductivity, salt-water solution with a salt content of 3.0 wt% was used as the fluid media and the liquid height in the large tank was 430 mm.

In this work, a wall source made of 0.5 mm diameter copper wire mesh was attached on one of the side-walls of the inner tank as shown in Fig. 3. During experiments, the source was connected to the negative pole of the DC supply to generate fine hydrogen bubbles in the inner tank (the building). The anode was made of a graphite plate with dimensions of 10 mm (wide)  $\times$  8 mm (thick)  $\times$  60 mm (long).

The buoyancy flux, which represents the strength of a buoyancy source, was evaluated as  $B_w = gQ_g(\rho - \rho_g)/\rho$ . Here,  $\rho_g$  is the density of hydrogen gas. The gas flow rate per unit area,  $Q_g$ , from the cathode was obtained by measuring the current flow through the system. The height of the stratification interface was measured by two rulers attached to the front wall of the inner tank.

#### 3.2. Qualitative observations

Fig. 4 shows a typical stratification induced by the vertical wall source with a buoyancy flux per unit area of  $2.28 \text{ cm}^2 \text{ s}^{-3}$ . The top opening was 0.5% of the total ceiling area. The figure shows essentially a two-layer stratification with a very weak stratification in the upper layer. On the right is the same figure at a reduced size in order to make the weak interface more visible. As indicated by the arrows in Fig. 4, the weak stratification interface declines slightly from the left to the right. It was observed that the weak interface is smeared in the region close to the wall source, as roughly delineated by the dashed lines in the rectangular region.

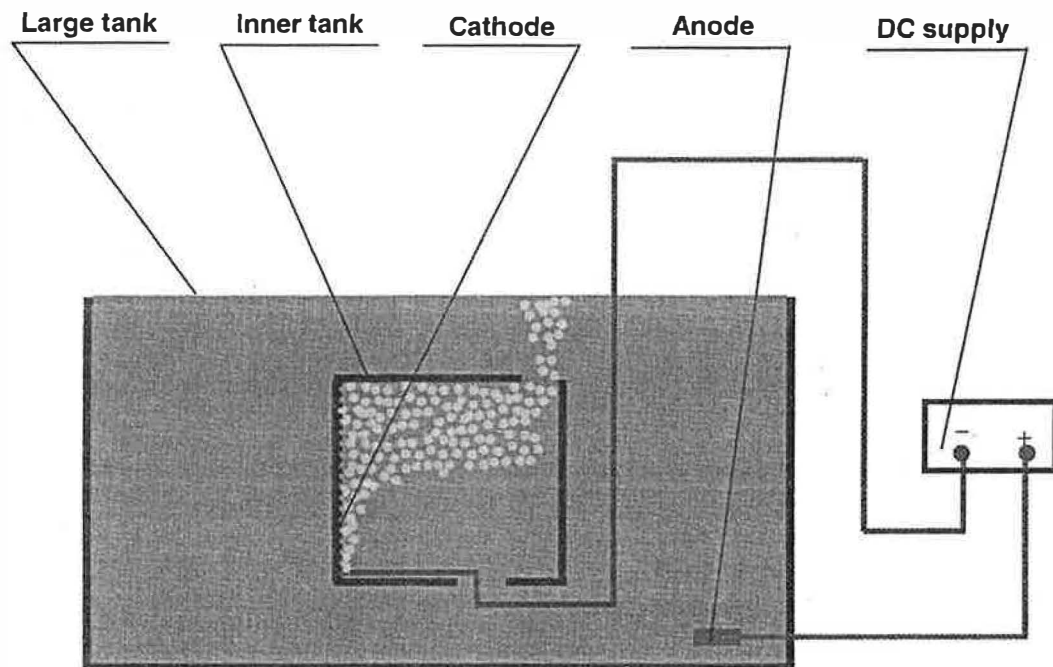


Fig. 3. Schematic view of the experimental system.

During the rising of a turbulent plume, fluid is entrained and carried upwards as long as the surrounding fluid is denser than the fluid in the plume. However, when the fluid around the plume is lighter than the outer layer of the plume, the outer layer fluid will slow down, eventually stop and leave (or peel off) the plume. Consequently, fluid de-entrainment occurs when the surrounding fluid is lighter than the outer layer of the plume.

In Fig. 4, the fluid in the delineated rectangular region is a mixture of the fluid in the middle layer and that in the top layer. Although no bubble void fraction has been measured in this work, it is most likely that the fluid density in this region varies vertically. During experiments, fluid de-entrainment was observed in this region, which indicates that the surrounding fluids are lighter than the outer layer of the plume. In contrast to the model of Linden et al. [1], the de-entrained fluid does not spread into the top layer, but mixes with the surrounding fluids and sinks down to a level with the same density in the middle layer, as shown in Fig. 4. It should be noted that fluid de-entrainment from the plume can occur at a range of heights in the rectangular region. The higher the de-entrainment position, the lighter the fluids de-entrained. Consequently, with the settlement of these de-entrained fluids, a distribution of fluid density with height is expected in the middle layer. At the lower region of the middle layer, these previously de-entrained fluids will be re-entrained into the plume.

At the same time, the remaining part of the plume, mainly the core of the plume, keeps rising into the top layer due to its momentum and the additional buoyancy flux from the wall source. Having peeled off its

outer layer near the interface between the middle and top layer, this core plume can again entrain fluid around it at the low region of the top layer.

From the above observations, it is seen that in the middle layer, fluid de-entrainment from the plume occurs in the upper region, while fluid entrainment occurs at the lower region, as shown in Fig. 4. It has also been observed that the depth of the middle layer decreases with an increase in the effective opening size, and the middle layer eventually disappears when the effective opening size is above a certain value. Observations in this work showed that the depth of the middle layer can be significantly different from that of both the bottom and the top layers. These experimental findings are in disagreement with those suggested by the model of Linden et al. [1], as shown in Fig. 2.

#### 4. Present model

In Linden's model, de-entrainment of the fluid in the plume into each layer occurs at the lower interface level. Consequently, the reduced gravity (and thus the density and the temperature) in each stratification layer should be approximately constant and undergo step changes between adjacent layers, as shown by the solid line in Fig. 5. However, both the experiments by Linden et al. [1] and Cooper et al. [2] suggested that there is essentially a two-layer stratification with an approximately linear density distribution in the upper layer. Multi-layer stratification, when it exists, is very weak. Linden et al. [1] suggested that a significant amount of vertical mixing may contribute to the smoothing out of the stratifications in the upper layer.

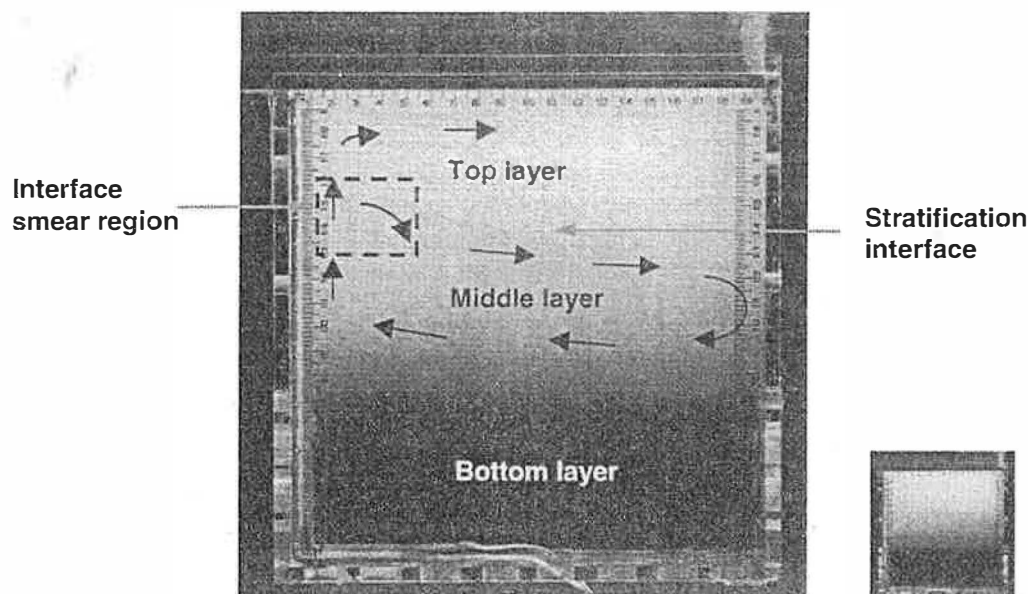


Fig. 4. Stratification induced by a continuous vertical wall source in a single-zone building.

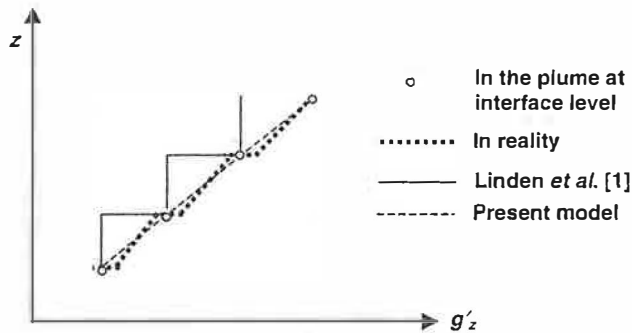


Fig. 5. Reduced gravity distribution in a building with a vertically distributed wall source.

Etheridge and Sanderberg [5] investigated a contaminant concentration distribution in an enclosure with a vertically continuous line source. They also observed that the fluid de-entrained at a high level sinks down to a low level with the same density and will be re-entrained by the plume at this low level. Chen and Cardoso [6] showed that when a buoyancy plume rises across a stepwise stratification interface, a fraction of the dense, lower layer liquid carried in the plume is de-entrained, spreads radially and sinks down to the low layer. The observations by Etheridge and Sanderberg [5] and Chen and Cardoso [6] are in accordance with the present experimental observations. Based on these experimental observations, a simple multi-layer stratification model is suggested in the following, as shown schematically in Fig. 6.

When the plume reaches a stratification interface, e.g. the interface between layer 2 and 3, part of the outer layer of the plume will be peeled off (or de-entrained) due to its relatively high density compared with that of the fluid in layer 3. The de-entrained fluid sinks down to a level with the same density in layer 2. At the lower region of layer 2, the previously de-entrained fluid will be re-entrained into the plume.

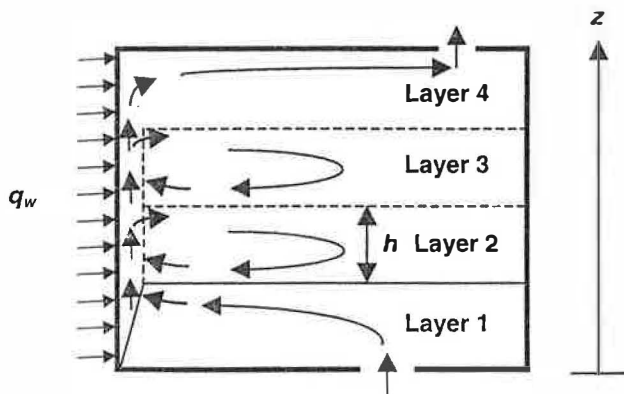


Fig. 6. The present multi-layer stratification model for displacement ventilation induced by a vertically distributed buoyancy source.

If we assume that the density is uniform in the plume at a fixed horizontal level and there is no fluid exchange across the interface outside the plume, then conservation of the buoyancy flux at any interface level,  $i$ , can be expressed by the following equation:

$$g'_{z,i} = \frac{B_w z_i}{Q} \tag{11}$$

The circles in Fig. 5 represent the reduced gravity in the plume at each interface level. Due to the entrainment and de-entrainment at each stratification layer, the distribution of the reduced gravity in the plume should not be linear along the vertical height. As shown in the rectangular region in Fig. 4, fluid de-entrainment can occur at a range of heights near the high interface level. The fluid de-entrained at high levels should be lighter than that de-entrained at low levels. The settlement of this de-entrained fluid results in a distribution of density in each layer outside the plume in reality, as schematically shown by the bold dotted line in Fig. 5.

The minimum possible density in a certain layer, say layer 3, is that in the plume leaving layer 3, and the maximum possible density in layer 3 is that in the plume entering from layer 2. Although both the maximum and minimum densities may not be achieved, the density changes between two adjacent layers (except between the bottom layer and layer 2) might not be significant and the multi-layer stratification, if it exists, is not distinctive. Consequently, the fact that fluid de-entrainment occurs at a range of heights near the high interface level and entrainment occurs at a low level within each stratification layer, effectively smooths out the multi-layer stratification. In this sense, the multi-layer stratification essentially reduces to a two-layer stratification with a weakly stratified upper layer.

Since the plume, fluid entrainment and de-entrainment in each layer (except the bottom and the top layers) are similar, the volume flux conservation requires an approximately equal depth for all these layers. It should be noted that a strict theoretical analysis for such a complex multi-layer stratification system is very difficult. In the following, a simplified analysis is carried out.

The reduced gravity of the outflow through the top opening is  $g'_H = B_w H/Q$  and the reduced gravity of the plume flow into the second layer is  $g'_h = B_w h/Q$ . Considering the weak stratification in the region above the bottom layer, we may approximate the reduced gravity above the bottom layer by a linear distribution, as shown by the dashed line in Fig. 5:

$$g'_z = \frac{B_w z}{Q} \tag{12}$$

For such a two-layer stratification system, the conser-

h/H

Fig. 7  
predi

vation of volume flux and Bernoulli's theorem can be expressed by the following two equations:

$$Q = u_1 a_1 = u_2 a_2 \quad (13)$$

$$\frac{u_1^2}{2c_1} + \frac{u_2^2}{2c_2} = \frac{B_w(H^2 - h^2)}{2Q} \quad (14)$$

Thus, the flow rate through the openings can be obtained:

$$Q = A_w^* \left[ \frac{B_w(H^2 - h^2)}{2Q} \right]^{1/2} \quad (15)$$

From Eqs. (7) and (15) we have:

$$\frac{A_w^*}{H} = F^{3/2} \xi^2 \left( \frac{2}{1 - \xi^2} \right)^{1/2} \quad (16)$$

where  $\xi = h/H$ .

The corresponding volume flow rate through the openings and the reduced gravity in the upper layer can be determined by Eqs. (15) and (12), respectively. The temperature distribution above the bottom layer can be obtained by the following relation:

$$g_z' = \frac{T_z - T_0}{T_0} g \quad (17)$$

From Eqs. (8), (9) and (16), it is seen that the interface position is exclusively determined by the geometrical parameters of the building and independent of the strength of the buoyancy source. This is consistent with the theoretical predictions for point and horizontal line sources of Linden *et al.* [1].

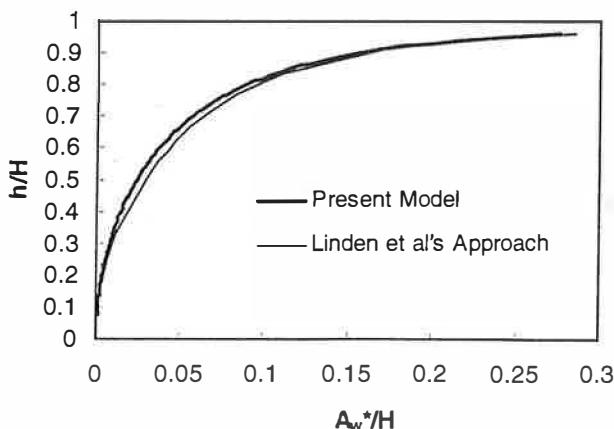


Fig. 7. Comparison of the dimensionless stratification interface depth predicted by Linden's model and the present model.

## 5. Results and discussion

Figs. 7 and 8 show comparisons for the dimensionless stratification depth  $\xi = h/H$  and the dimensionless volume flux  $Q/B_w^{1/3}H^{4/3}$  as predicted by the model of Linden *et al.* [1] and the present model. It is seen that these two models give very close values of the stratification depth and ventilation flow rate, with the predictions by the present model slightly higher (generally less than 10%). Consequently, both models may be applicable to the evaluations for the bottom layer depth and ventilation flow rate. However, it should be noted that there are several major differences between the present model and the model suggested by Linden *et al.* [1], viz:

- As shown in Figs. 2 and 6, the flow directions in layers 2 and 3 in Linden's model and the present model are opposite due to the differences in the de-entrainment and entrainment regions.
- The present model shows that the fluid de-entrainment occurs at a range of heights near the upper interface level and entrainment occurs at the lower level within each stratification layer effectively smooths out the multi-layer stratification.
- Linden's model predicts that the depth of the bottom layer must be equal to other layers except the top layer. The present model suggests that both the bottom layer and the top layer thickness may be different from those of other layers.

As discussed above, the experimental observations in this work support the present model.

Fig. 9 shows the experimental results obtained for the bottom layer stratification depth with the source strengths  $B_w$  of 1.71 and 2.28  $\text{cm}^2 \text{s}^{-3}$ , respectively. The predictions by the two stratification models and the experimental results of Cooper *et al.* [2] were also

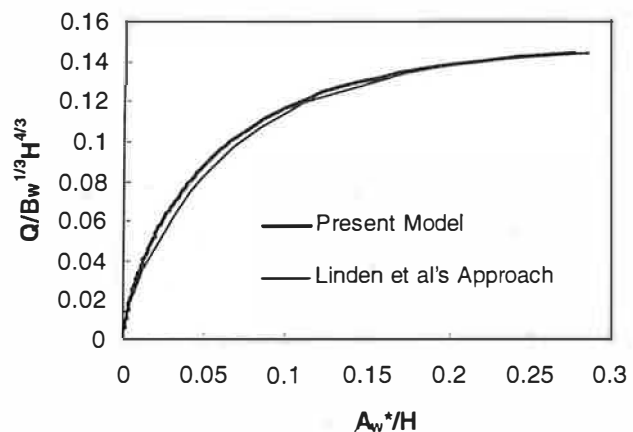


Fig. 8. Comparison of the dimensionless volume flux per unit width through openings predicted by Linden's model and the present model.

included for comparison. The values of  $c_1$ ,  $c_2$  and  $\alpha$  used here were 0.61, 0.61 and 0.102, respectively.

It is seen that the source strength has a small or indiscernible influence on the stratification interface depth, which is in agreement with the theoretical predictions. It is also seen that the experimental results obtained in this work are in good agreement with the theoretical predictions by both Linden's model and the present model.

On the other hand, significant differences were found between the experimental results obtained in this work and those by Cooper et al. [2] who used a salt-bath modelling system. In the experiments by Cooper et al. [2], the buoyancy flux was generated by supplying salt solution through a vertical porous wall. An examination of the results of Cooper et al. [2] showed that the volume flux of the salt solution itself was about half the volume flux through the bottom opening. In this situation, the assumption of  $z\Delta Q \ll Q$  is no longer valid. In addition, the introduction of salt solution through the porous wall may give rise to additional driving pressure, since the initial velocity of the salt solution could be relatively significant if the permeability of the wall is small.

The effects on the interface level of the additional volume flux and driving pressure due to the introduction of salt solution are complex. For example, the additional volume flux below the stratification interface results in the reduction of the inlet velocity through the bottom opening. Thus, a reduced flow resistance at the bottom opening should give rise to a higher interface level. On the other hand, however, the additional volume flux in the upper layer results in an increase in the outlet flow velocity and thus gives rise to a lower interface level. Similarly, the additional driving pressures due to the introduction of salt solution below and

above the neutral pressure level also affect the interface level in an opposite way. The exact influence of the additional volume flux and driving pressure depends on the magnitude of the two opposite contributions.

In the present work, the buoyancy flux was generated by hydrogen gas bubbles. The volume flux of the gas bubble per unit area generated by the wall source can be expressed by the following equation:

$$Q_g = \frac{B_w \rho}{g(\rho - \rho_g)} \approx \frac{B_w}{g} \quad (18)$$

Considering the volume increase per unit area due to a heat source  $\Delta Q = q_w / \rho C_p T_0 = B_w / g$ , the bubble volume flux in the present modelling system closely represents the volume increase due to a heat source. This might be the reason for the good agreement between the experimental results obtained in this work and the theoretical predictions. It should be noted that for the salt-bath system, using a high-concentration salt solution may reduce the influence of the additional volume flux and the additional driving pressure due to the introduction of the salt solution. Investigations using the salt-bath system with high-concentration salt solutions are needed for the further verification of the theoretical predictions presented in this work.

## 6. Conclusions

A simple multi-layer stratification model is suggested for displacement ventilation in a single-zone building driven by a heat source distributed uniformly over a vertical wall. It was shown that fluid de-entrainment occurs at a range of heights near the high interface level and entrainment occurs at the low level within each stratification layer, effectively smoothing out the multi-layer stratification. In contrast to the multi-layer model available in the literature, the present model suggests that both the bottom and top layer depth may be different from those of other layers. It was also shown that the experimental results obtained in this work using the fine-bubble technique are in good agreement with the theoretical predictions.

## References

- [1] Linden PF, Lane-Serff GF, Smeed DA. Emptying filling boxes: the fluid mechanics of natural ventilation. *J Fluid Mechanics* 1990;212:309-35.
- [2] Cooper P, Mayo GA, Sorensen P. Natural ventilation of an enclosure with a distributed buoyancy source applied to one vertical wall. In: *Proceedings of the 6th International Conference on Air Distribution in Rooms*, Stockholm, Sweden, 14-17 June, 1998.
- [3] Morton BR, Taylor GI, Turner JS. Turbulent gravitational con-

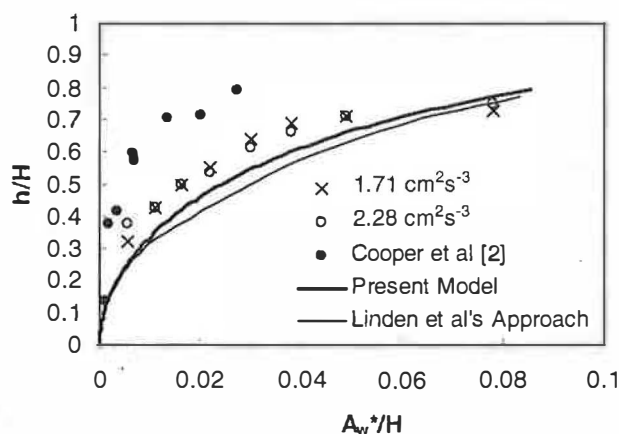


Fig. 9. Comparison between the experimental results of the bottom layer depth obtained in this work, theoretical predictions and the experimental data by Cooper et al. [2].



- vection from maintained and instantaneous sources. *Proc Royal Society A* 1955;234:1–23.
- [4] Chen ZD, Li Y, Mahoney J. Experimental modelling of buoyancy-driven flows in buildings using fine-bubble technique. *Building and Environment*, in press.
- [5] Etheridge DW, Sanderberg M. In: *Building ventilation: theory and measurement*. New York: Wiley, 1996. p. 459–64.
- [6] Chen MH, Cardoso SSS. The mixing of liquids by a plume of low-Reynolds number bubbles. *Chemical Engineering Science* 2000;55(14):2585–94.